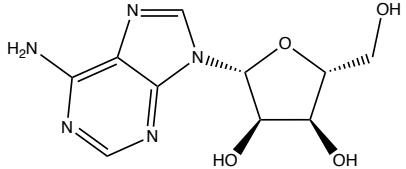
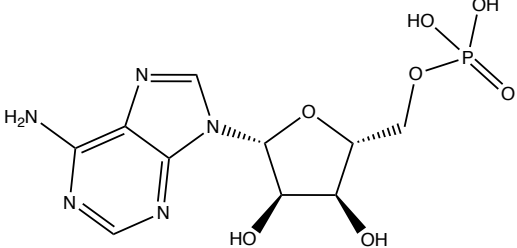
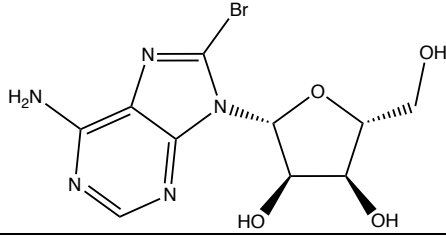
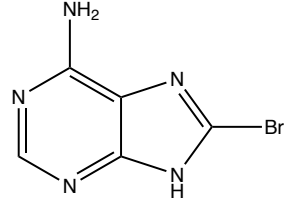
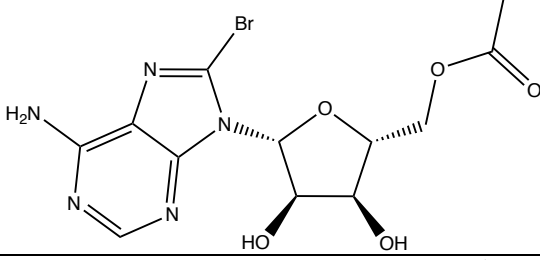
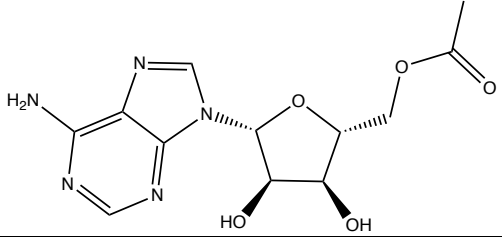
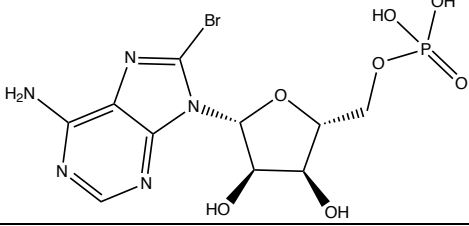
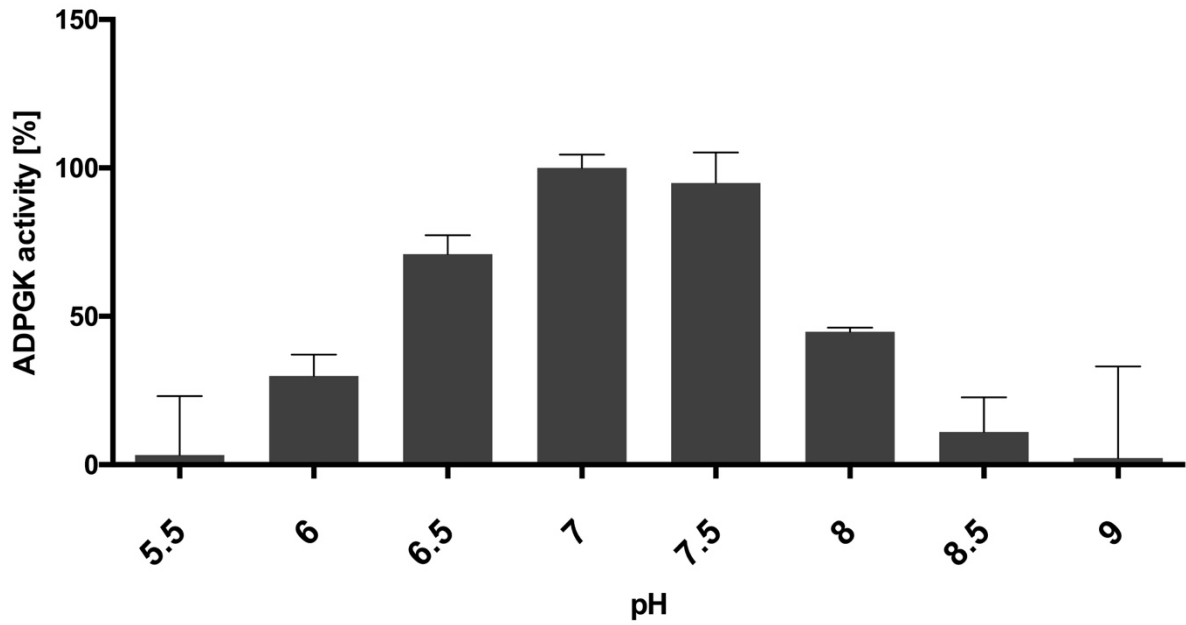


## Supplementary information.

**Table S1.** Structures of adenosine analogues utilized in this study.

Compound name	Structure
Adenosine	
Adenosine monophosphate	
8-bromoadenosine	
8-bromo-9H-purin-6-amine	
8-bromoadenosine acetate	
5-O-acetyladenosine	
8-bromoadenosine monophosphate	

A



B

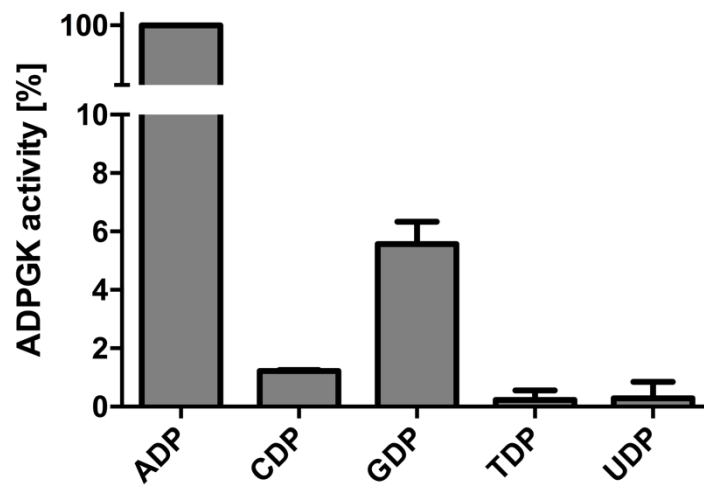


**Figure S1. hADPGK properties** (A) activity pH dependence (B) Substrate specificity towards different dinucleotides.

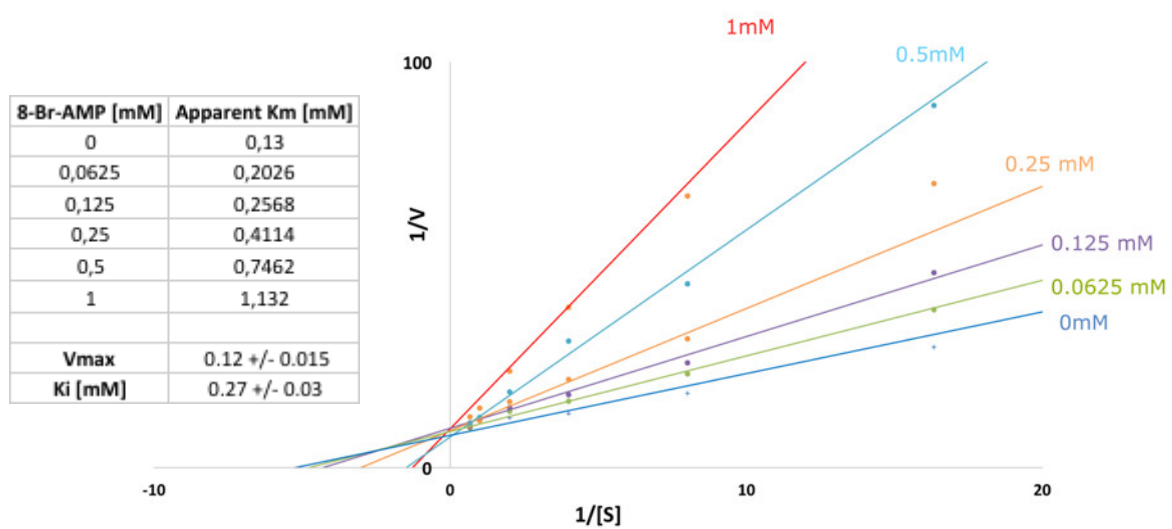


**Figure S2.** Lineweaver-Burk plot of hADPGK kinetics in the presence of 8-Br-AMP.

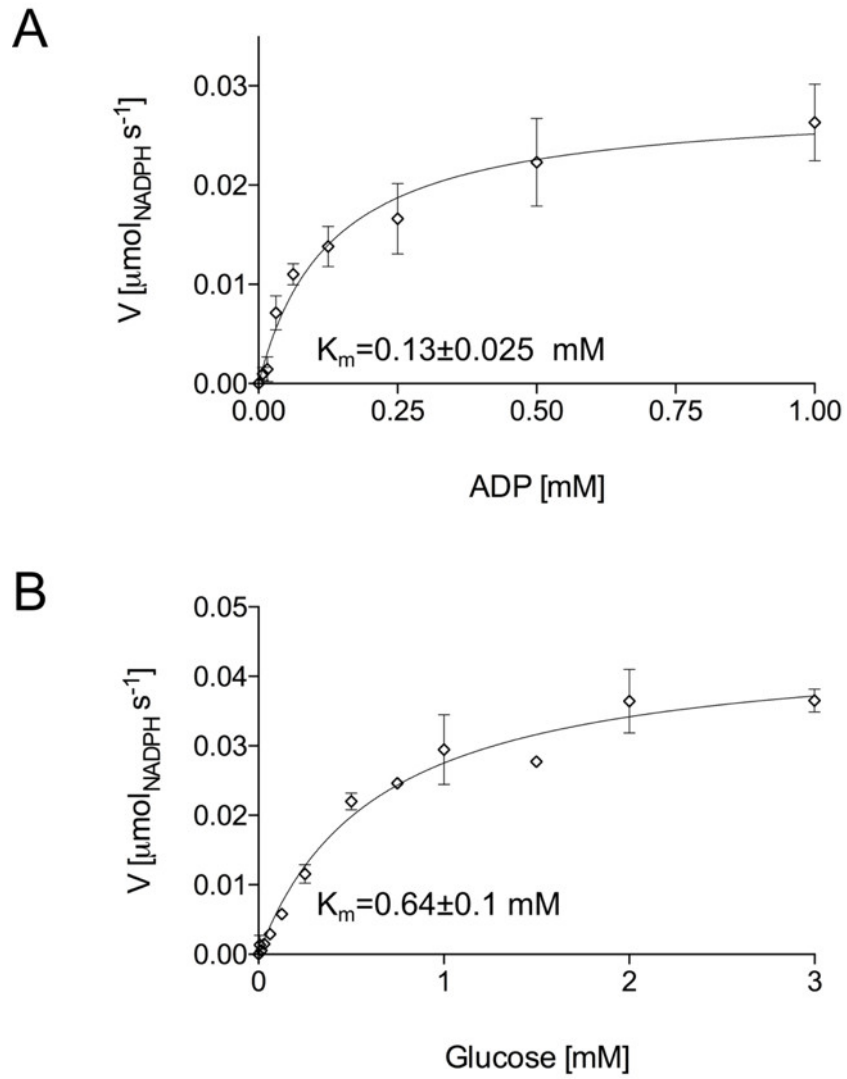
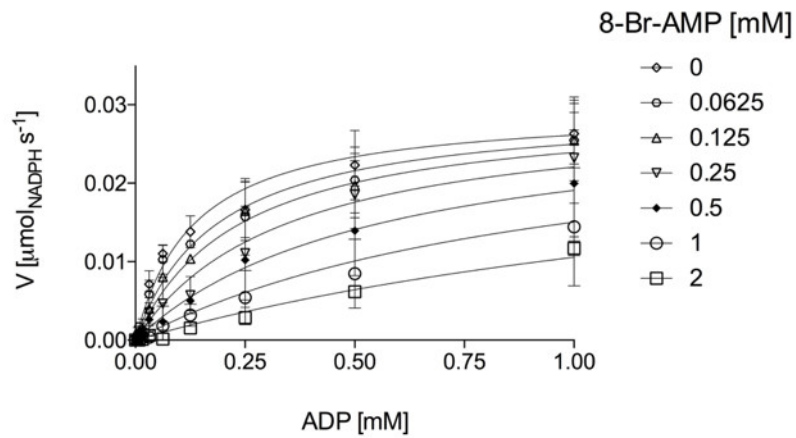


**Figure S3.** Enzymatic characterization of phADPGK.  $K_m$  and  $V_{\text{max}}$  determination for ADP (A) and glucose (B).

A



8-Br-AMP [mM]	Apparent Km [mM]
0	0,1292
0,0625	0,1502
0,125	0,2213
0,25	0,5204
0,5	0,5986
1	1,389
2	~ 28,95
<b>Vmax</b>	0.031 +/- 0.003
<b>Ki [mM]</b>	0.16 +/- 0.017

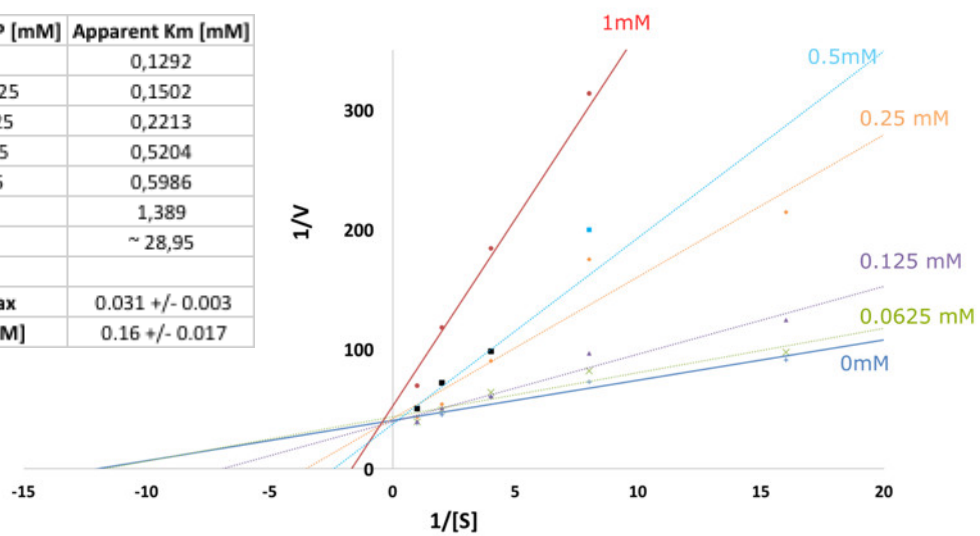


**Figure S4.** A. Inhibition of phADPGK by 8-Br-AMP. B. Lineweaver-Burk plot of phADPGK kinetics in the presence of 8-Br-AMP.

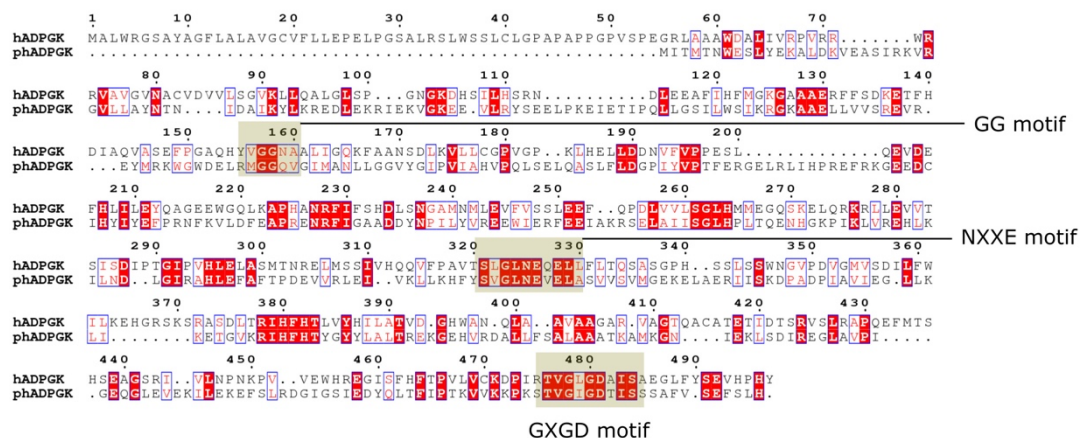
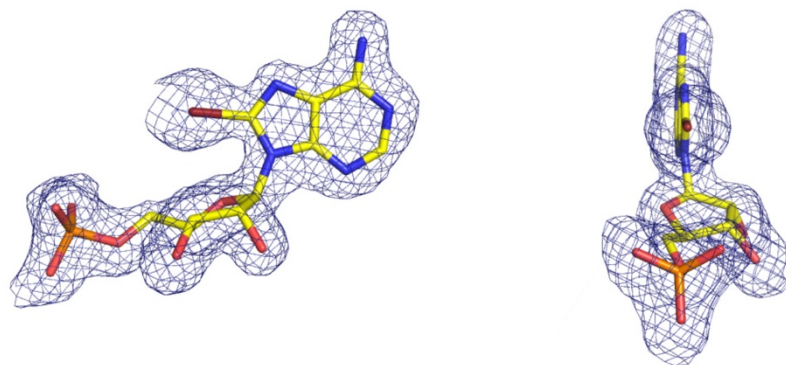


**Figure S5.** Sequence alignment of human and archaeal ADPGK. Highly conserved substrate binding motifs are highlighted. Overall sequence identity is 25%.

A



B

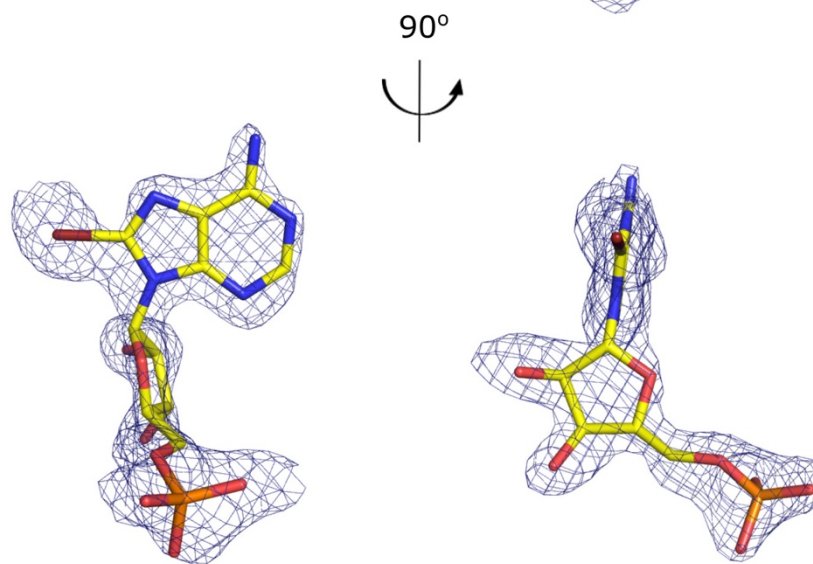


**Figure S6.** Simulated annealing  $F_o-F_c$  composite omit maps ( $3\sigma$ ) calculated for 8-Br-AMP within the active site (A) and additional 8-Br-AMP molecule (B).

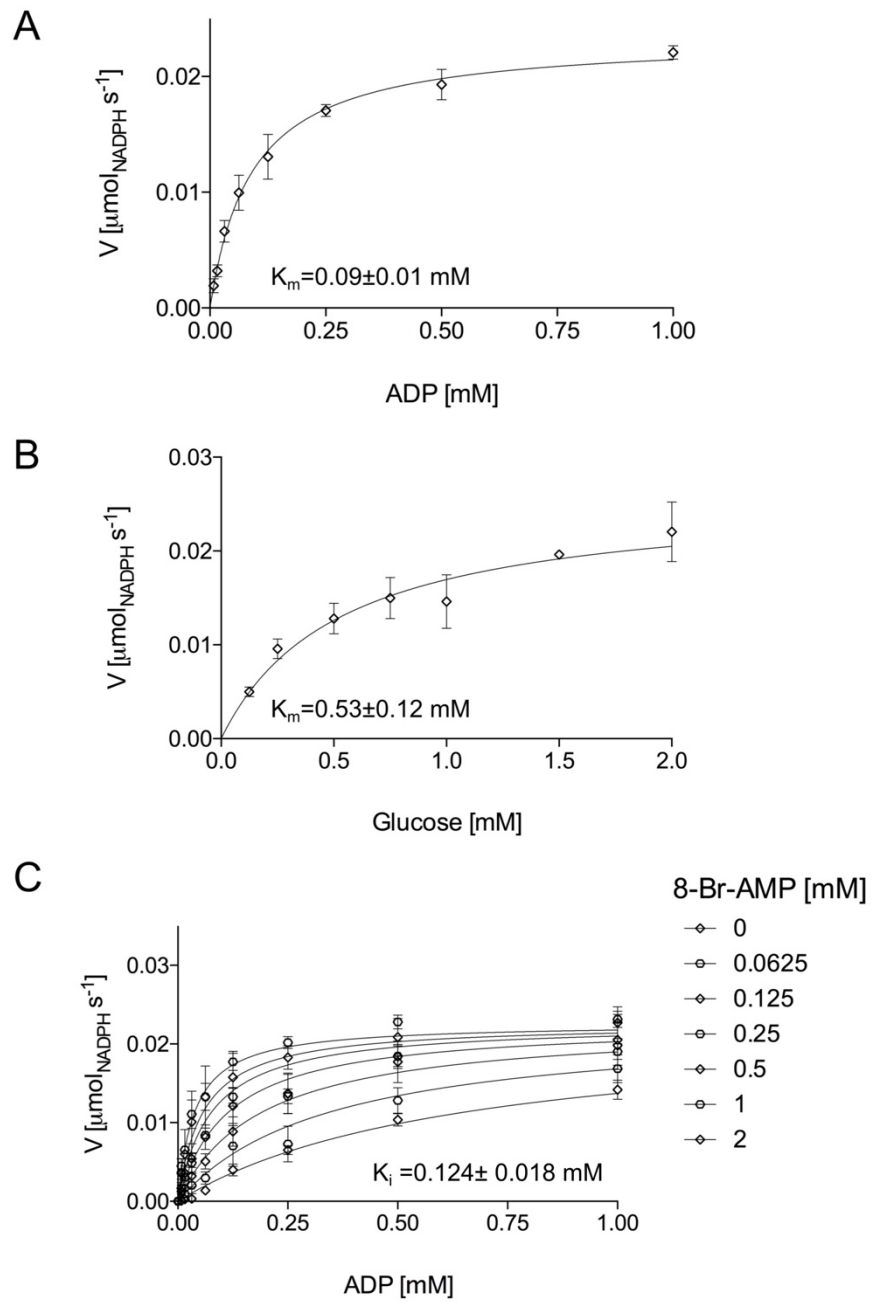


**Figure S7.** Enzymatic characterization of phADPGK F272A.  $K_m$  and  $V_{\text{max}}$  determination for ADP (A) and glucose (B). Inhibition of phADPGK F272A by 8-Br-AMP.



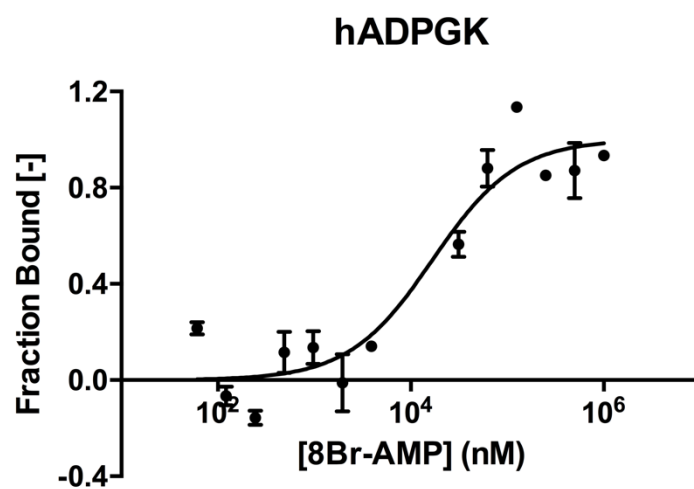


**Figure S8.** Binding of 8-Br-AMP to hADPGK analyzed by Microscale Thermophoresis.

$K_d=16.55 \pm 4.78 \mu\text{M}$

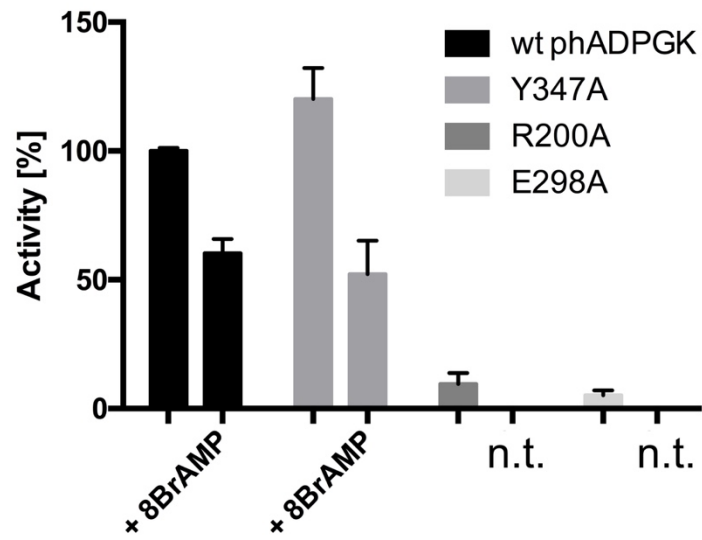


**Figure S9. Effect of amino acid substitutions on the phADPGK activity.** The substitution of Tyr347 for alanine did not cause any significant changes either in the protein activity or inhibition by 8-Br-AMP (1mM), however the substitutions of Arg200 and Glu298 led to inactivation of phADPGK (n.t. – not tested).

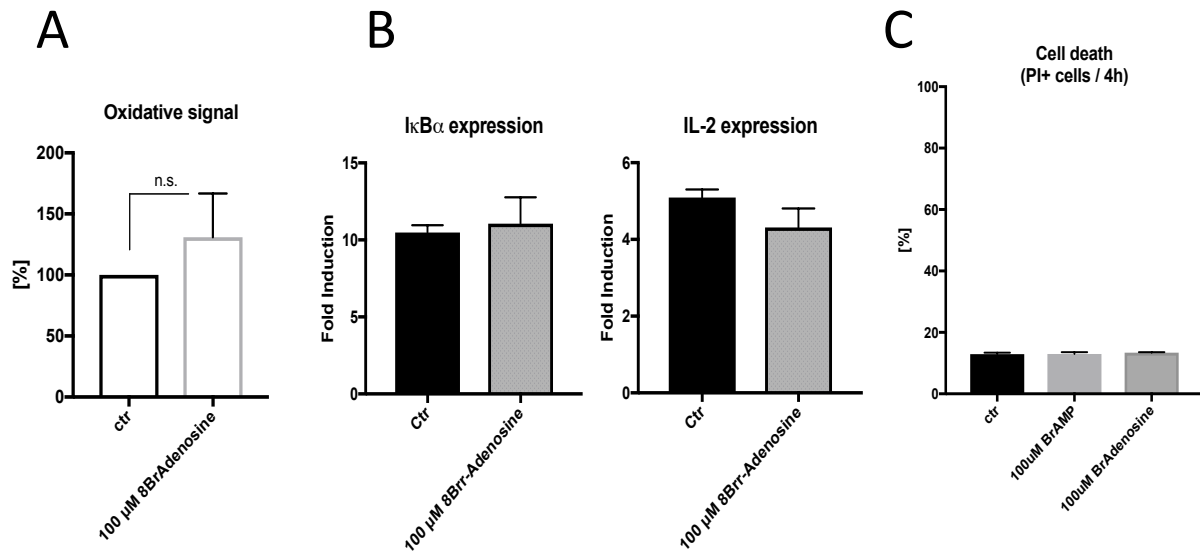


**Figure S10. 8-Br-adenosine does not inhibit T cell activation-induced ROS generation and subsequent NF-κB-dependent gene expression.** (A), Jurkat T cells stained with H<sub>2</sub>DCF-DA and 30 min pre-treated with 100 μM of 8-Br-adenosine were activated by PMA treatment (1 h) and the ‘oxidative signal’ was measured by FACS (mean values +/- SD). Cumulative results of three independent technically triplicated experiments are shown (mean values +/- SD). Statistical significance was calculated by single sample t test (ctr set up to 100%). (B), 8-Br-adenosine-pre-treated Jurkat T cells (30 min) were activated by PMA/ionomycin treatment for 1 h. Next, IL-2 and IκBα gene expression was assayed by RT-PCR (mean values +/- SD). (C), Jurkat T cells were treated with 100 μM of 8-Br-AMP or 8-Br-adenosine for 4 hours and cell death was assayed by FACS measurement of PI+ cells (mean values +/- SD).